Temporal-spatial Meteorological Variability of Drought and Flood Characteristics using in situ observations and Multi-satellites Reanalysis Products over the Republic of Djibouti From 1901 to 2021

Abdi-Basid ADAN

Correspondence mail: abdi-basid@outlook.com

Abstract:

The Spatial-temporal studies of drought and flood events was conducted for the first time, using data from 35 rainfall stations, distributed over the 6 districts of the Republic of Djibouti. The drought assessment is based on the SPEI and SPI indices at three time scales (3, 6 and 12 months) during the period 1961 to 2016. Accuracy of the very high resolution satellite product reanalysis was conducted using (CHIRPS), (ERA-5), (PERSIANNCDR), Terra Climate, (CHELSA) for precipitation and (CHIRTS), (CFR), (ERA-5) and Terra Climate for Minimum and Maximum temperature. The main results are summarized as follows:

Keywords: drought assessment; SPI; SPEI; VCI; NDVI; reanalysis, Djibouti

1. Introduction

The Republic of Djibouti is a smallest nation in the Horn of Africa, bounded to the north by Eritrea, to the west and south by Ethiopia and to the southeast by Somalia (Figure 1). Due to its geostrategic position, Djibouti is a major crossroads for international maritime trade. On the strength of its political stability, on the commercial silk route crossing Africa, Djibouti will represent the gateway to the rest of continent. Recommended by the World Meteorological Organization (WMO), the standardized precipitation index (SPI/SPEI) is used to characterize, in real time, drought throughout the world [1,2]. In a spatiotemporal approach, these indices describe the evolution, frequency and severity of extreme weather events (drought and floods)

[3]. Due to global warming, the variation in the rate of precipitation in recent decades makes several regions vulnerable to worsening drought [4]. Studies in Ghana, Malawi, South Africa and Ethiopia have revealed a longer-term impact of drought on rural livelihoods (access to water and livestock) [5]. Christensen et al. showed a decrease in rainfall in northern and southern Africa, an increase in rainfall in the Ethiopian highlands, and an increase in the frequency of floods and droughts [6]. In addition, in the East African region, the countries of Somalia, Ethiopia, Uganda and Kenya have been affected by recurrent episodes of drought phenomena, especially in the period from 2010 to 2011 [4]. For the other countries in Africa, South Africa, Malawi and Ghana were severely affected by drought between 1982 and 1984. Despite the scarcity of water, the use of non-potable water, the appearance of epidemics of the salubrity of waters make many victims. [10]. Statistical studies have shown that the equatorial and temperate climate types (climates A and C) had approximately twice as many drought events as the arid and polar climate types (climates B and E) [15].

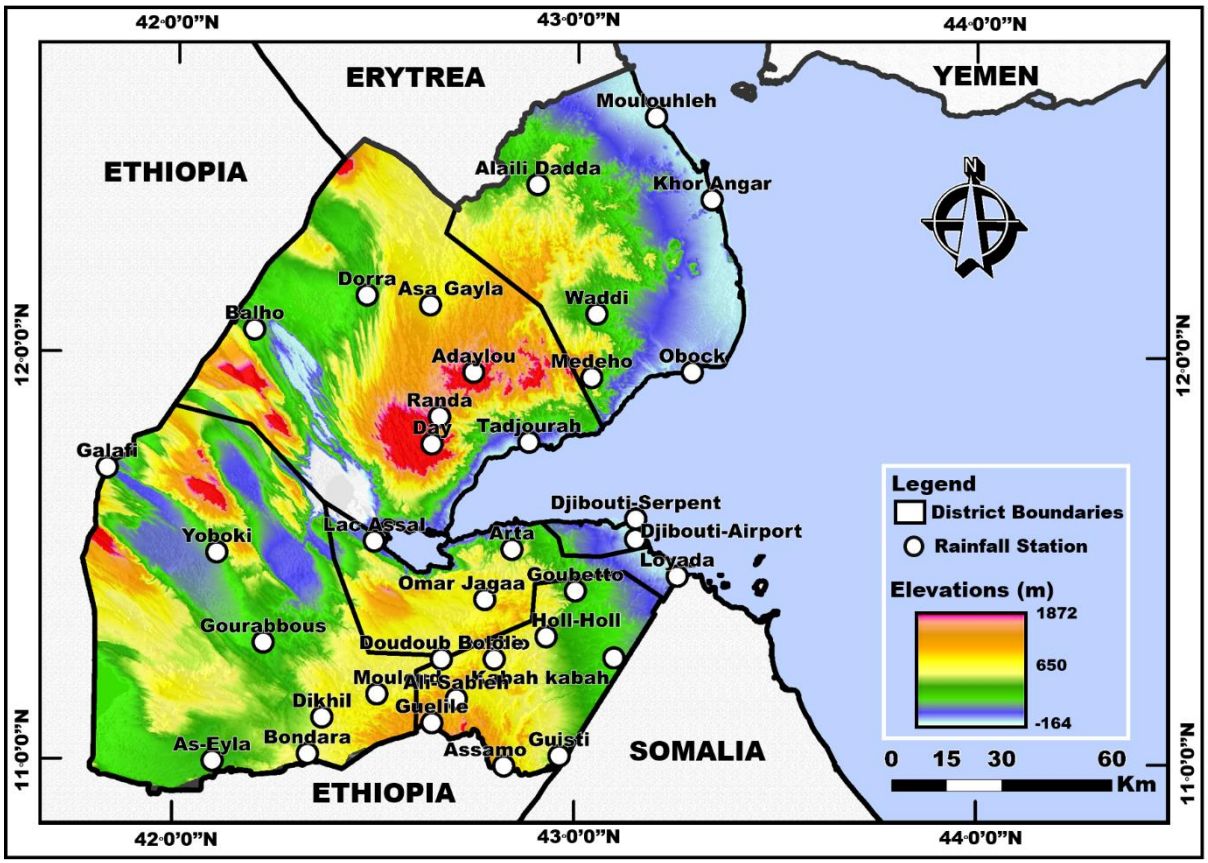

FIGURE 1. Location map showing the topographical elevation (m) and the locations of the 35 stations with annual mean rainfall at each station.

The climate of East Africa, in general, is of the semi-arid type with irregular variation in precipitation. Regionally four seasons can be defined during the year (JF, MAM, JJAS and OND.) The long rainfall season is considered the months of March-April-May (MAM). The season during which the precipitation reaches its lowest level is the months June-July-August-September (JJAS). This phenomenon can be explained with climate change events such as ELNINO and the sea surface temperature anomaly (SST), which influences precipitation patterns (Figure 2). Due to a decrease in rainfall in southern Ethiopia, in February-May and June-September, the year 2009 was marked by an exceptionally widespread drought, since that observed in 1984. [7]. The drought had a considerable impact on population mobility in the rural highlands of Ethiopia with 10% of adult males annually [8]. Lack of seasonal rainfall induces loss of crops and livestock and often leads to severe food shortages and psychological

stress among affected people [9]. Drought assessments based on the VCI and SPI showed that Eritrea had been exposed to moderate to extreme drought conditions over the past 18 years. The low rainfall was mainly attributed to the decreasing trend of vegetation and increasing drought conditions in the semi-arid region [11]. Moreover, the longest drought in Somalia occurred from March 1989 to July 1992, lasting 41 months, then from December 2004 to May 2007 and from May 2011 to January 2013 lasting respectively 30 months and 21 months. In contrast, the 2011 drought exacerbated a famine in southern Somalia and affected nearly 3.1 million [13,14].

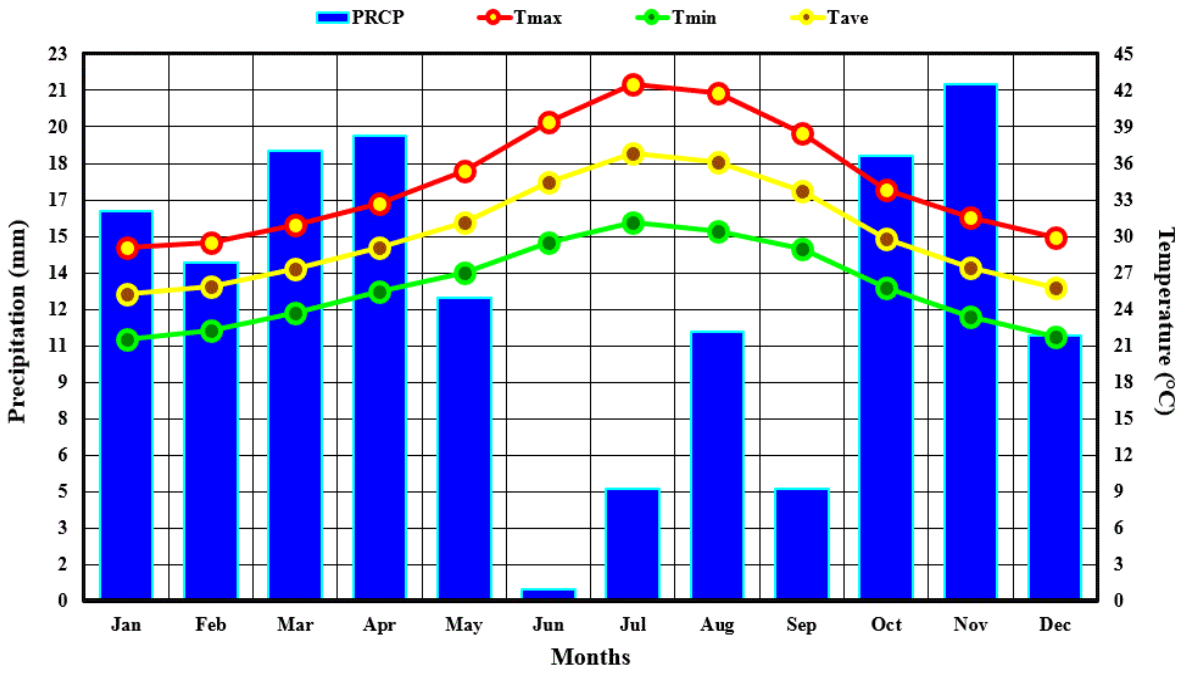

FIGURE 2. Ombrothermic Diagram for Monthly Temperature and Precipitation variation over the period 1953 - 2019.

2. Materials and Methods

2.1 Study Area

The Republic of Djibouti is located in the Horn of Africa, bounded by Eritrea to the north, Ethiopia to the west and southwest, and Somalia to the southeast (Figure 1). The Köppen-Geiger climate classification of the region ranges from "hot desert" to "semi-arid" with a low precipitation regime and an average annual precipitation of 150 mm (climate type codes BWh and BSh, respectively) [32,33]. Two seasons predominate: a cool season (winter) of October to April with a monthly average temperature of 20–30 C and a hot season (summer) from May to September with an average monthly temperature of 30 to 45 C. In summer, the year the equatorial westerly wind zone dominates and the average temperature increases between 30 and 45 C with a high rate of evapotranspiration amounting to 2000 mm per year [7,8].

2.2 Data Description

2.2.1 Observational Data

Times Series Monthly precipitation data collected from 35 meteorological stations covers the period from 1961 to 2021. Figure 1 shows the spatial distribution in the Republic of Djibouti. In addition to rainfall data, the Djibouti Airport meteorological station has monthly minimum and maximum temperature data for the period from 1953 to 2017. The station withy which could be modeling drought since 1901 is the Djibouti Serpent rainfall station. Table 1 listed the names, the geographical coordinate location of the 35 meteorological stations and the average annual rainfall. The database is compiled by the Djibouti National Meteorological Agency (Agence Nationale de la Météorologie de Djibouti (ANMD), in French).

2.2.2 Multi-Satellite Reanalysis Data

Table 2. Summary of the Reanalysis precipitation and temperature product reanalysis gridded datasets.

PRODUCT	DEVELOPER	SPATIAL EXTENT	SPATIAL RESOLUTION	TEMPORAL COVERAGE
CHIRPS	USGS & CHC scientists	Global	0.05°	1981–2022
PERSIANN CDR	University of California	Global	0.25°	1983–2021
ERA5	European Center for Medium Range Weather Forecast	Global	0.25°	1979–2022
Terra Climate	University of Idaho	Global	0.042°	1958–2020
CHELSA v2.1	Swiss Federal Research Institute	Global	30 arc sec (≅0.01°)	1979–2018
CHIRTSv1.0	U.C., Santa Barbara	Global	0.05°	1983–2016
CFS Reanalysis	Environmental Modeling Center at NCEP, USA	Global	0.2°	1979–2022

2.3 Methods and Metrics

2.3.1 Standardized precipitation index

The long-term characteristic drought monitoring, rainfall times series variation are a fundamental component. The Standardized Precipitation Index (McKee et al., 1993) is one of the most commonly used methods, dues of its numerous advantages (Svoboda et al., 2012). SPI is used to measure, in particular, the long-term precipitation anomalies and especially expresses the possibility of quantifying the rarity of precipitation (McKee et al., 1995). The monthly precipitation time series are fitted by a gamma probability distribution function. The result of cumulative distribution is transformed into cumulative distribution function of the standard normal distribution []. Indeed, the normalized probability distribution makes it possible to compare both the drought and humidity of the study area. The inverse normal function is applied to produce the cumulative probability for the SPI results. We consider x as the cumulative monthly precipitation values over the period of (1, 3, 6, 12 months, etc.), for the calculation of the function of the gamma probability density G(x) as follows:

$$G(x) = \frac{1}{\beta^{\epsilon}\Gamma(\varepsilon)} \int_0^x x^{\epsilon-1} e^{-\frac{x}{\beta}} dx, x > 0 \quad (1)$$

where x represents the cumulative value of precipitation, ε and β are scale and shape parameters, $\Gamma(\varepsilon)$ indicates the Gamma function for ε. Considering the possible extreme condition of absence of rainfall during a month. The Gamma distribution is transformed as follow:

$$H(x) = pr + (1 - pr)G(x) \quad (2)$$

where pr indicates the probability of precipitation, which is equal to zero. Thus, the result of the SPI calculation is obtained with the following equations:

$$SPI = S\left(t - \frac{c_0 + c_1 t + c_2 t^2}{1 + d_1 t + d_2 t^2 + d_3 t^3}\right) \quad (3)$$

$$t = \begin{cases} \sqrt{\ln(1/H(x)^2)}, & if\ 0 < H(x) \leq 0.5 \\ \sqrt{\ln(1/1 - H(x)^2}, & if\ 0.5 < H(x) < 1 \end{cases} \quad (4)$$

where the constant values are c0 = 2.51558, c1 = 0.80286, c2 = 0.01039, d1 = 1.43279, d2 = 0.189290, and d3 = 0.001390.

2.3.2 Standardized Precipitation Evapotranspiration

The temporal assessment of drought characteristics based on the SPEI index requires, together with precipitation, the potential evapotranspiration (PET). This double entry of climate data makes it possible to take into account the variations of drought in a warming climate (Wang et al., 2014). The water balance equation is fitted with the logarithmic logic models as follows:

$$F(x) = \left[1 + \left(\frac{\varepsilon}{x - \eta}\right)^{\beta}\right] \quad (5)$$

where x represents water balance equation and β, ε, and η indicate the scale, shape, and locality constraints, respectively. Thus, the SPEI index is calculated with the following equations:

$$SPEI = W - \frac{c_0 + c_1 W + c_2 W^2}{1 + d_1 W + D_2 W^2 + D_3 W^3} \quad (6)$$

$$W = \begin{cases} \sqrt{-2\ln\left(F(x)\right)}, & if\ 0 < F(x) \leq 0.5 \\ \sqrt{-2\ln\left(1 - \mathrm{F(x)}\right)}, & if\ 0.5 < F(x) < 1 \end{cases} \quad (7)$$

Similar to the Equation (3), Equation 6 has the same coefficients for c0, c1, c2, d1, d2, and d3. The calculation of SPEI can be conducted at various time scales, ranging from 1 month to 24 months, which depicts different drought type (Vicente Serrano et al., 2010). The classes of SPI and SPEI are given in Table 1 [].

Table 3. Drought classification SPEI values

SPI/SPEI classifications	Catégories
≤ -2.0	Extremely Dry
− 1.99 – -1.5	Severely Dry
− 1.49 – -1.0	Moderately Dry
− 0.99 – 0.99	Near Normal

1.0 – 1.49	Moderately Wet
1.5 – 1.99	Severely Wet
≥ 2.0	Extremely Wet

The method is considered the best equation for PET estimation in all climates and is calculated as fellow []:

$$PET = 0.0023(T_{max\_}T_{min})^{0.5}(T_{mean} + 17.8)Ra \quad (8)$$

where Tmax, Tmin, and Tmean indicate the maximum, minimum, and mean temperature (°C) and Ra shows the extraterrestrial radiation (MJm−2 day−1).

3. Results

3.1 Data Quality Control

Time series data are evaluated first for quality control. In this process, missing, outlier values and homogenization process of observations from each station are examined. Missing values in the precipitation series from meteorological stations have been quantified. Almost a global rate of 0.523% of missing values are determined. The raingauge stations of Djibouti-Serpent, Alaili-Dadda Gourabbous and Galafi have over the period 1961 to 2021 0.098%, 0.082, 0.0014% and 0.0014% of missing rate value in the monthly observations, respectively (Table 1). Further, for each meteorological station with missing values at least of 6 years (represents a 10% of dataset) were completed using the multiple imputation method. This process proved to be more efficient and more accurate than simple imputation in completion of missing values [1, 2]. In addition, the completed values are controlled by comparing with those of the nearest station in order to assess the consistently of the estimation [3].

On the other hand, the identification of outliers in the database, for each gauge rain station, two methods are conducted for high rigorous examination. The first process allow to define a threshold of non-extreme and extreme outliers for each station, with which not be required for correction procedure [1, 2]. A second approach has been defined in order to sufficiently justify

for applying of any procedure treatment of outlier. In this study, we are assumed a maximum threshold of 350 mm/month, which all value higher than, is considered erroneous value and corrected with the nearest station observation [1, 3]. The extreme outlier threshold is lower for each station than the maximum threshold of 350 mm/month. However, the Djibouti serpent station exceeds this threshold with 544 mm/month in April 1989. This erroneous value has been readjusted to 344 mm/month. For the same month, we observed with the Djibouti airport station (close to the Djibouti serpent station), a value of 332 mm/month. Since 1961, the maximum precipitation was reported, most recently in November 2019, with 338 mm/month.

Additionally, the analysis of the homogeneity on the monthly time series of precipitation, maximum and minimum temperature data was examined. 35 meteorological stations were evaluated over the period 1961-2021. To explore the homogeneity of precipitation and temperature time series, a threshold of significance level of 5% were considered [1,3]. In this regard, five homogeneity tests were applied, Pettitt's test, Standard Normal Homogeneity test, Buishand's test, the Autocorrelation test and the von Neumann test [1,2,4]. Inhomogeneity results from at least two different tests were sufficient to identify homogeneous data. 11 stations were tested as inhomogeneous. Thus, two homogenization methodologies were adapted to select the best one. The double mass curve method and climatol tools available with R software [1,2,3]. The results of climatol homogenization change the interannual variation gap and do not correspond to the observed reality. The application of the Double Mass Curve method was not enough to homogenize the non-homogeneous stations. Therefore, we will take into account the inhomogeneity of the observations [4].

Multi-scale monthly Drought variability

La corrélation entre SPEI et SPI de 3, 6 et 12 mois est réalisé pour les stations du district de Djibouti (Airport and Serpent). Les résultats montrent que la corrélation de Spearman varie entre 0.328 à 0.596 pour les trois échelles de temps de 3, 6 et 12 mois. La méthode Kernel a été employée pour pouvoir compléter les résultats de SPI pour la période de 2017 à 2021 de la station de Djibouti-Serpent (Table **4**).

Table 4. The Mann-Kendall test and Spearman's rank correlation of SPI-3 and SPEI-3 for Djibouti-Airport and Djibouti-Serpent stations.

Djibouti-Airport (1961-2021)	**Rho correlation**	**P-value**
SPEI-3 vs SPI-3	0.509	< 0.0001
SPEI-6 vs SPI-6	0.561	< 0.0001
SPEI-12 vs SPI-12	0.596	< 0.0001
NDVI vs SPI-3		
NDVI vs SPI-6		
NDVI vs SPI-12		
Djibouti-Serpent (1901-2021)	**Rho correlation**	**P-value**
SPEI-3 vs SPI-3	0.141	< 0.0001
SPIk-3 vs SPEI-3	0.423	< 0.0001
SPIk-3 vs SPI-3	0.255	< 0.0001
SPEI-6 vs SPI-6	0.161	< 0.0001
SPIk-6 vs SPEI-6	0.388	< 0.0001
SPIk-6 vs SPI-6	0.247	< 0.0001
SPEI-12 vs SPI-12	0.259	< 0.0001
SPIk-12 vs SPEI-12	0.328	< 0.0001
SPIk-12 vs SPI-12	0.500	< 0.0001
NDVI vs SPI-3		
NDVI vs SPI-6		
NDVI vs SPI-12		
NDVI vs SPEI-3		
NDVI vs SPEI-6		
NDVI vs SPEI-12		

Le résumé des tendances de Man Kendall des indices de SPI, SPEI, NDVI et SEDI est présenté dans le tableau 5. La tendance de la sécheresse baisse plus légèrement avec l'échelle de temps de 3 mois par rapport aux 6 et 12 mois. D'autre part, on note une baisse annuelle des indices de NDVI et SEDI durant la même période de 2000 à 2021

(Table 5). Le résultat montre que la même tendance est observée dans les indices de SPI, contrairement au SPEI pour la station de Djibouti Airport.

Table 5. Trend Man Kendell of annual variation over the period 2000-2021.

	Slope	P-value	R^2
NDVI-Serpent	-3.43e-03	**0.00**	0.72
SEDI-Serpent	-6.39e-03	0.62	0.02
SPI-3-Serpent	-2.15e-02	0.22	0.16
SPI-6-Serpent	-3.75e-0.2	0.06	0.30
SPI-12-Serpent	-5.910e-02	**0.017***	0.44
NDVI-Airport	-6.201e-04	0.18	0.15
SPI-3- Airport	-4.167e-02	**0.03**	0.36
SPI-6- Airport	-4.81e-02	**0.02**	0.27
SPI-12- Airport	-7.017e-02	**0.01**	0.36
SPEI-3- Airport	0.038	**0.025**	0.26
SPI-6- Airport	3.317e-02	0.086	0.20
SPI-12- Airport	3.06e-02	0.074	0.18

*Bold value is related to the significant P-value.

La durée de Moderately dry de SPI-3 représente 164 months, le deuxième phénomène le plus longue observé après le normal (992). Neanmoins, l'indice de SPEI-3 montre une durée de 58 mois (Table 6).

Table 6. The Duration, severity, and intensity occurrence of the dry and wet events over the Djibouti airport station over the period 1961-2021.

	SPI-3				SPEI-3			
	Duration	**Severity**	**Intensity**	**Frequency**	**Duration**	**Severity**	**Intensity**	**Frequency**
Extremely Wet	45	46.526	2.326	0.561	20	54.801	2.383	0.645
Very Wet	53	44.578	1.715	0.729	26	53.527	1.673	0.897
Moderately Wet	91	83.892	1.234	1.906	68	44.635	1.24	1.009
Near Normal	992	-18.121	-0.034	14.938	533	0.466	0.001	14.49
Moderately Dry	164	-70.711	-1.219	1.626	58	-48.564	-1.184	1.149
Severely Dry	23	-34.821	-1.658	0.589	21	-42.989	-1.791	0.673
Extremely Dry	0	-2.135	-2.135	0.028	1	-64.405	-2.385	0.757

Table 7. The Duration, severity, and intensity occurrence of the dry and wet events over the Djibouti-Serpent station over the period 1901-2021.

	SPI-3				SPEI-3				SPIK-3			
	D	S	I	F	D	S	I	F	D	S	I	F
Extremely Wet	33	109.352	2.43	3.099	43	73.889	2.239	2.273	43	106.88	2.485	2.961
Very Wet	76	90.263	1.703	3.65	47	132.527	1.744	5.234	47	82.152	1.748	3.237
Moderately Wet	129	111.687	1.227	6.267	103	159.277	1.235	8.884	103	125.623	1.22	7.094
Near Normal	972	5.75	0.006	68.32	1108	-56.23	-0.058	66.942	1108	-29.053	-0.026	76.309
Moderately Dry	98	-196.90	-1.20	11.295	126	-117.946	-1.204	6.749	126	-148.57	-1.179	8.678
Severely Dry	50	-38.726	-1.68	1.584	15	-85.606	-1.712	3.444	15	-23.427	-1.562	1.033
Extremely Dry	36	0	--	0	0	-88.292	-2.453	2.479	0	0	--	0

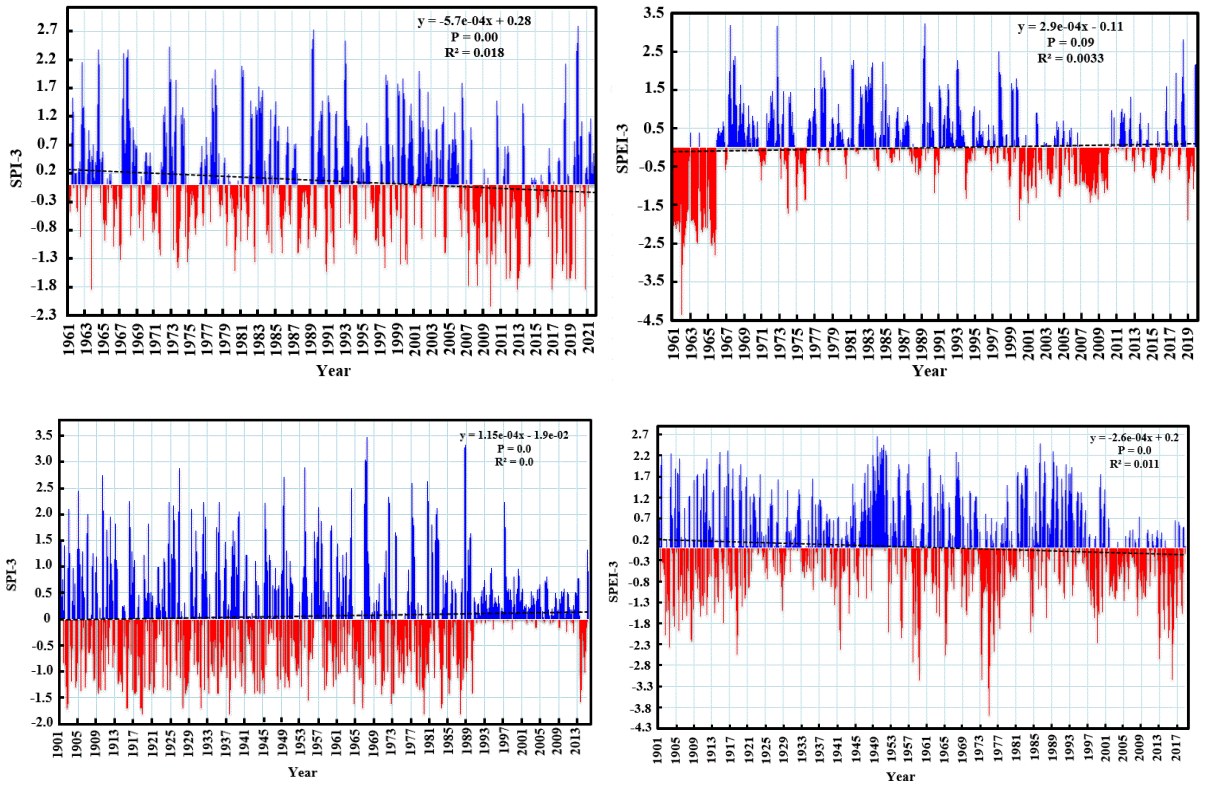

Figure 3. Linear trend of dry and wet event for SPI-3 and SPEI-3 using Mann-Kendall test over the Djibouti-Airport (up) and Djibouti-Serpent (down) meteorological station.

3.3 Regionalization Drought using SPI over the republic of Djibouti from 1961 to 2021.

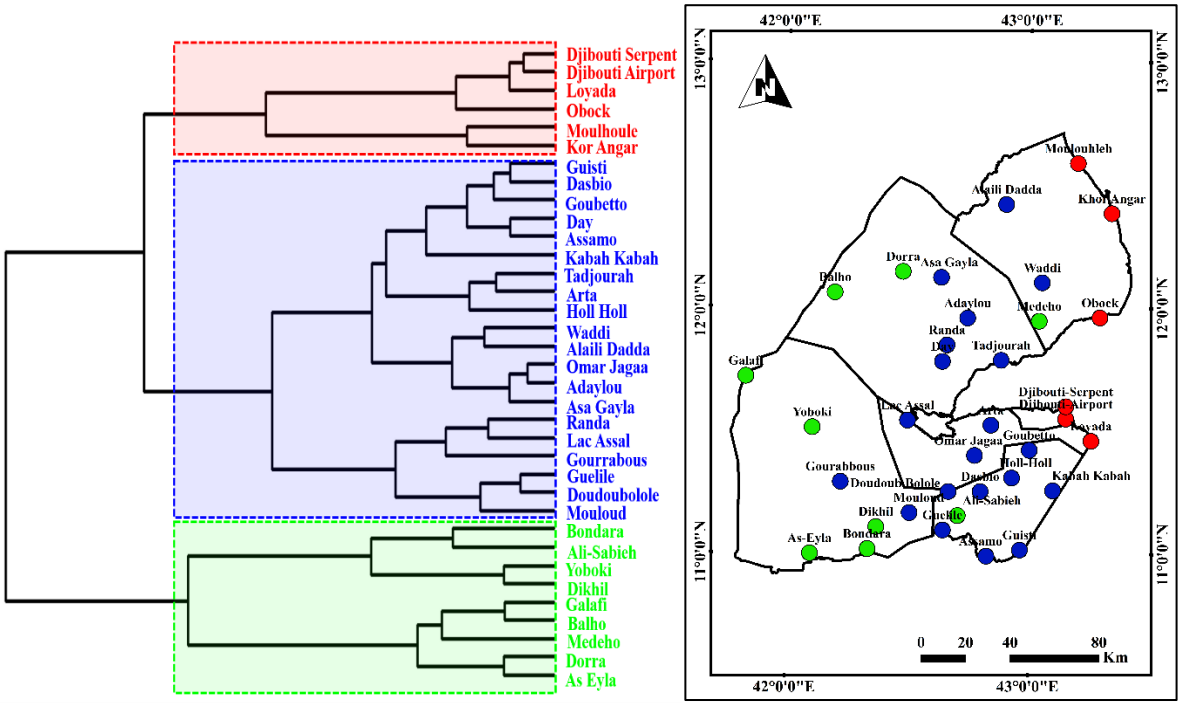

238

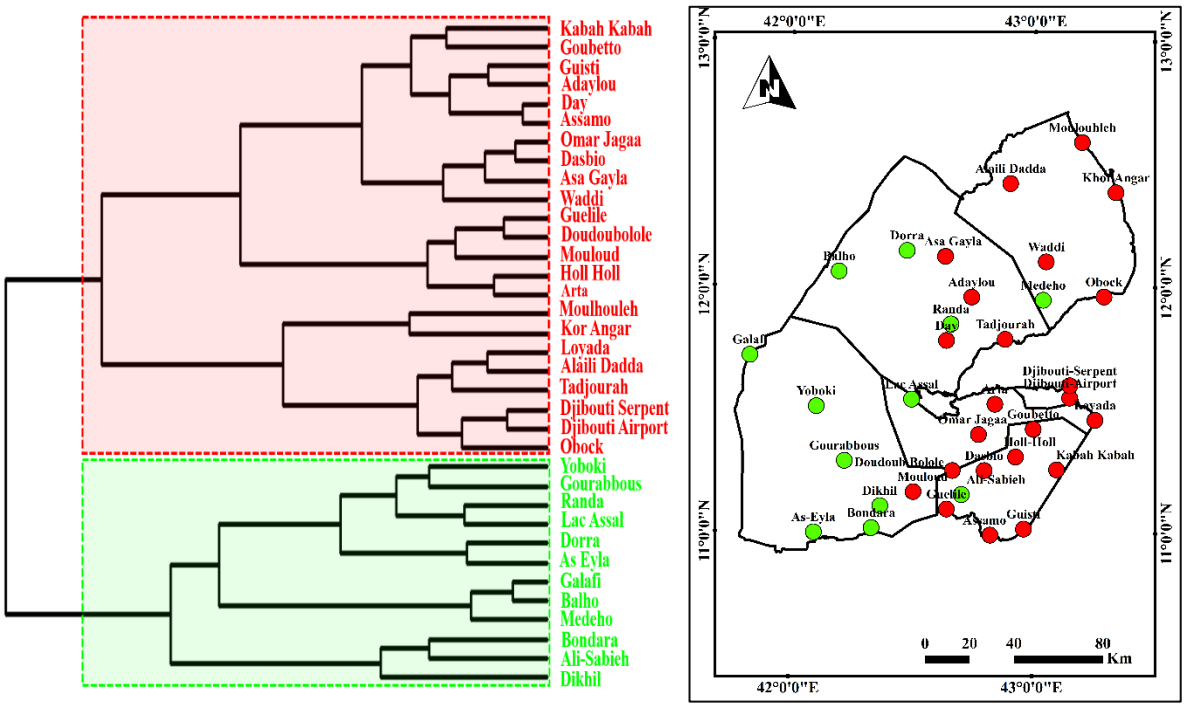

239

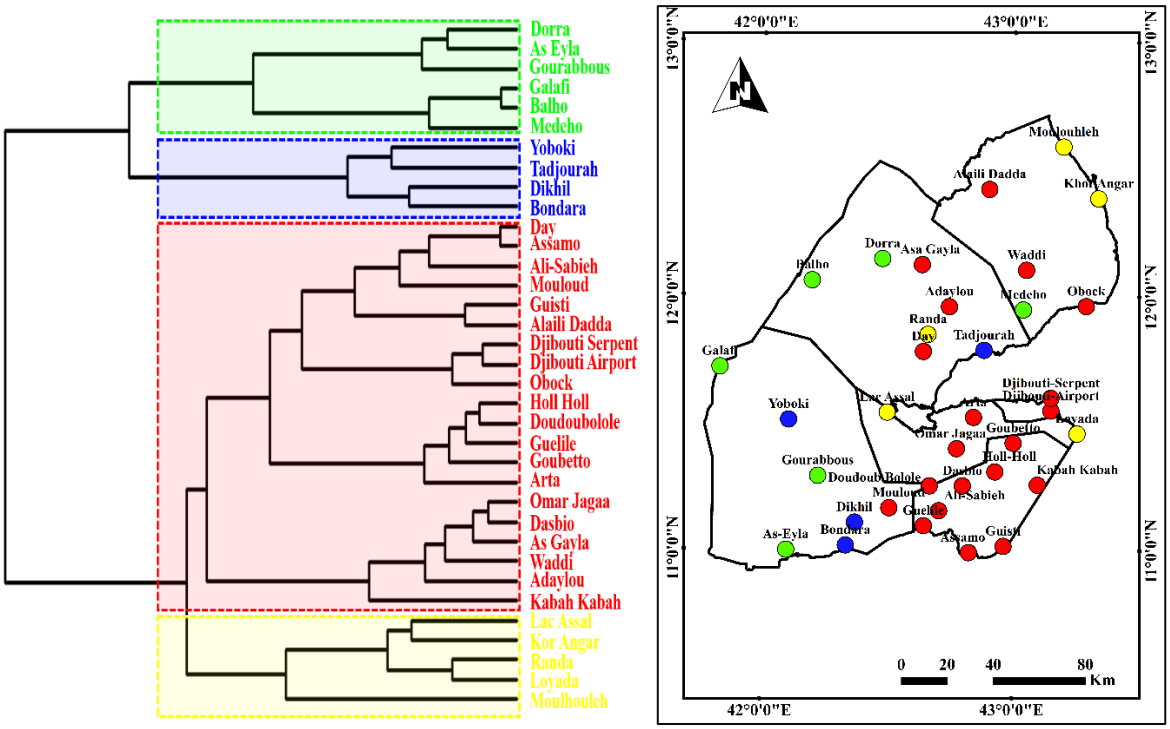

240

241 **Figure 4.** Dendrogram diagram (left) and Mapping of spatial (right) variability of SPEI
242 drought index clustering between stations using three time scale-3-6-12 over the period 1961
243 to 2021.

244 The spatial study of drought was conducted using Ascending Hierarchical Classification. The
245 *NbClust* package was used to determine the optimal number of clusters for each SPI time scale.
246 The results show 3, 2, and 4 regions for SPI-3, SPI-6, and SPI-12 months, respectively (Figure
247 4). The regionalization based on the SPI-3 index is the most geographically interpretable. The
248 coastal zone contrasts with the green zone, while the blue zone is intermediate. However, three
249 stations are poorly distributed geographically (Table 8).

250 The correlation analysis of the three groups with each of these stations shows that Medeho
251 station is more correlated with the central region (0.63) than with the western region (0.60).
252 The same applies to the Ali-Sabieh station. The Gourabbous station is slightly more correlated
253 with the central region. However, it should be noted that further studies are needed to better
254 clarify the heterogeneity of these three stations in relation to their regional positions (Table 8).

255
256
257
258
259

Table 8. Comparison of Corrected Three homogeneous regions for spatial pattern Drought over the Republic of Djibouti from 1961 to 2021 (The black dashed line demarcates the three regions).

Clusters	Statistics	East	Center	West
Number of station	**---**	**6**	**21**	**8**
Coloration	**---**	**Red**	**Blue**	**Green**
Rainfall (mm/month)	Min	0	0	0
	Max	344	254	166
SPI-3 months	Min	-2.13	-3.57	-3.79
	Max	3.91	4.57	4.24
SPI-6 months	Min	-2.98	-5.26	-5.05
	Max	4.03	4.22	4.19
SPI-12 months	Min	-2.9	-5.38	-6.84
	Max	4.08	4.62	3.97
Rho Spearman correlation of SPI-3 months				
SPI-3 Medeho	***[1]	---	**0.63**	0.60
SPI-3 Ali-Sabieh	***	---	**0.62**	0.56
SPI-3 Gourabbous	***	---	0.74	**0.75**

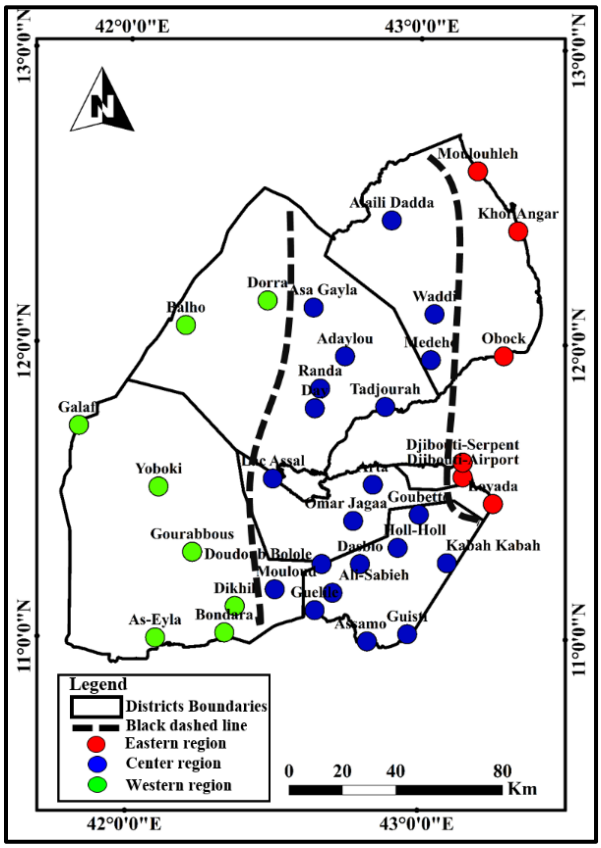

[1]*** Significant at 1%

3.3.1. Characteristics of drought in each station

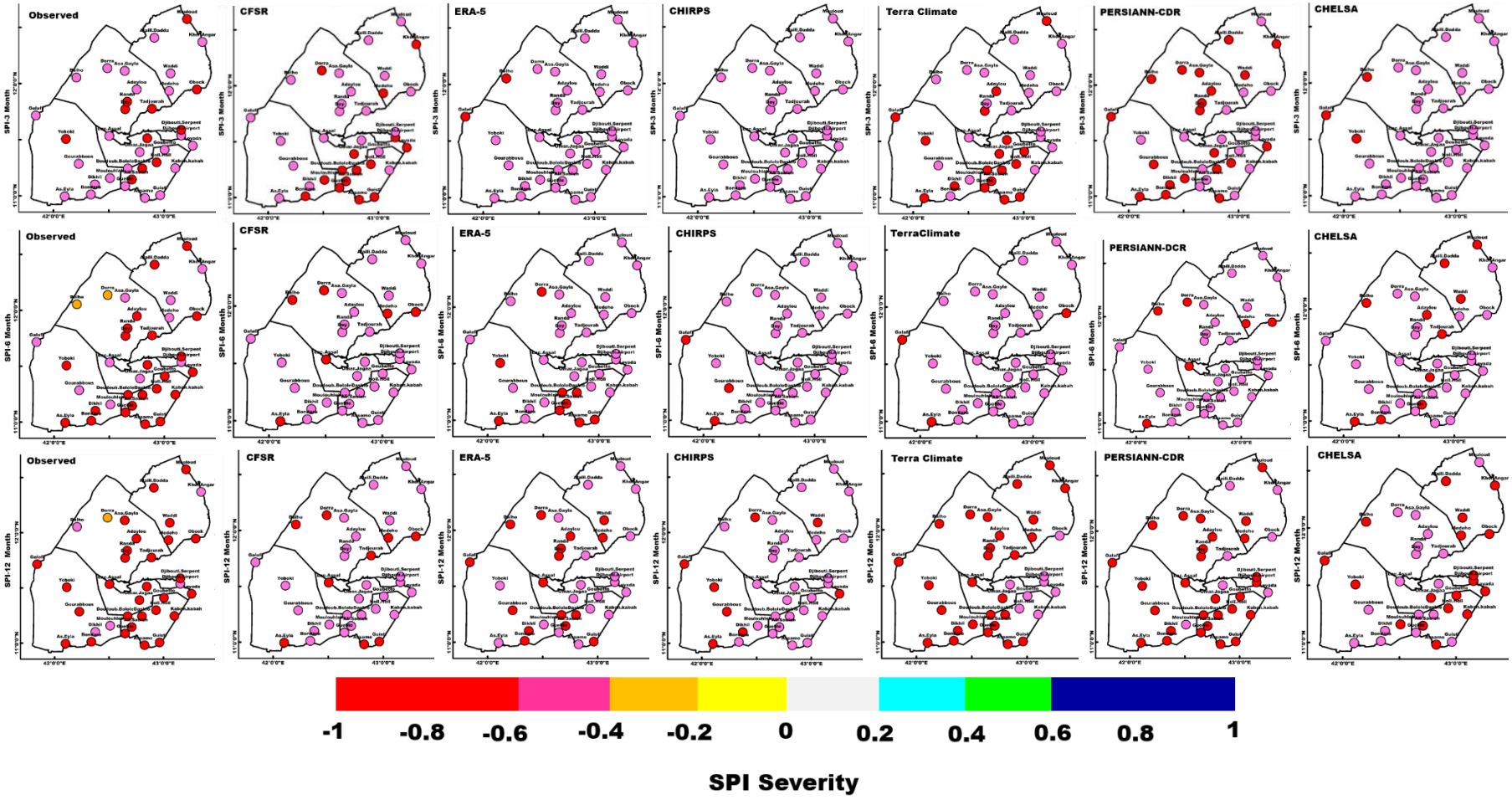

Figure 5. Spatial pattern of monthly drought- severity based on the standardized precipitation index (SPI) estimated in Republic of Djibouti during 1983-2021 at times scale 3, 6 and 12 months.

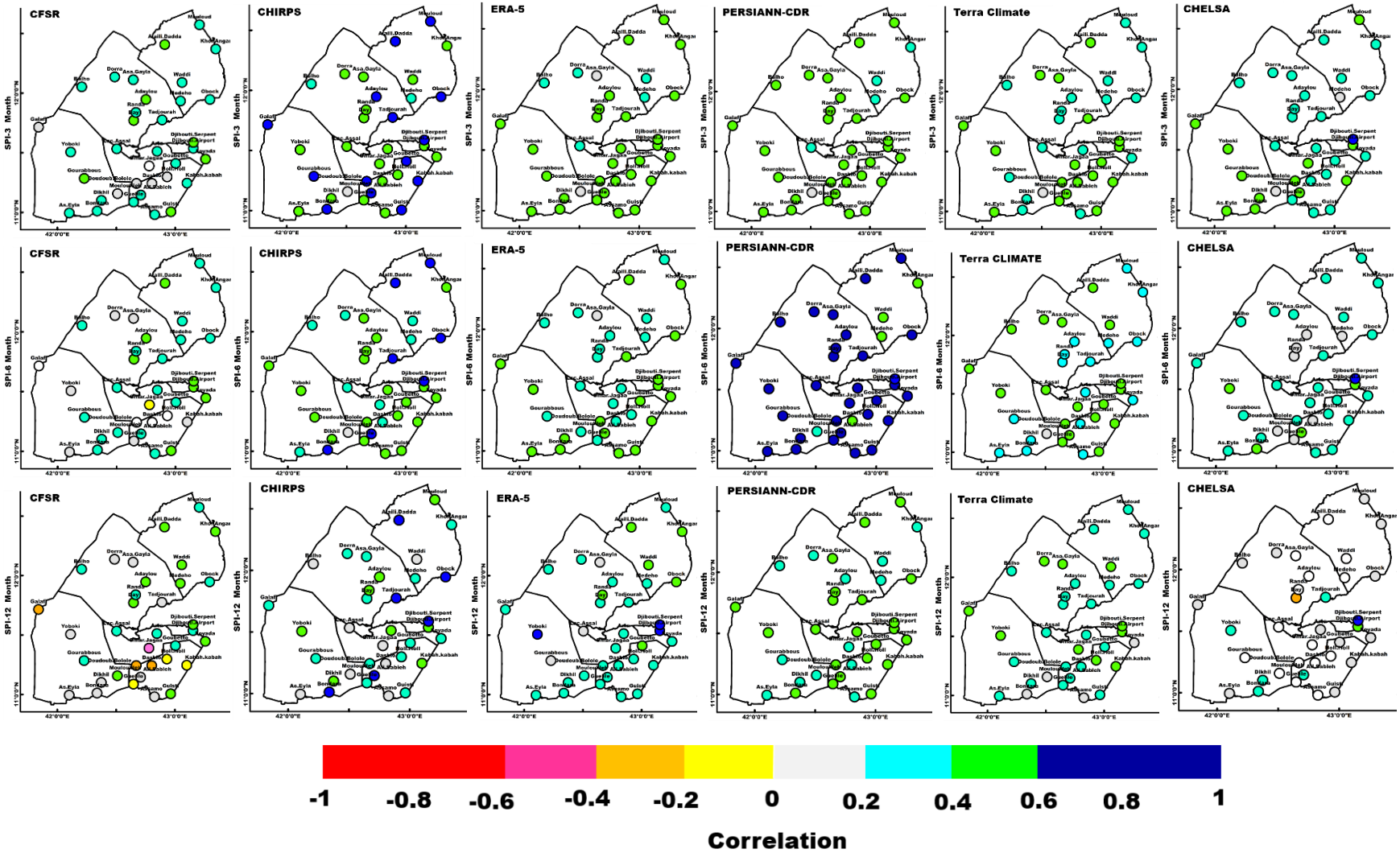

Figure 6. Spatial pattern of correlation of estimated monthly drought indices (3, 6, 12 month timescales) assessed from reanalysis products with the in situ observation over The Republic of Djibouti during 1983-2021.

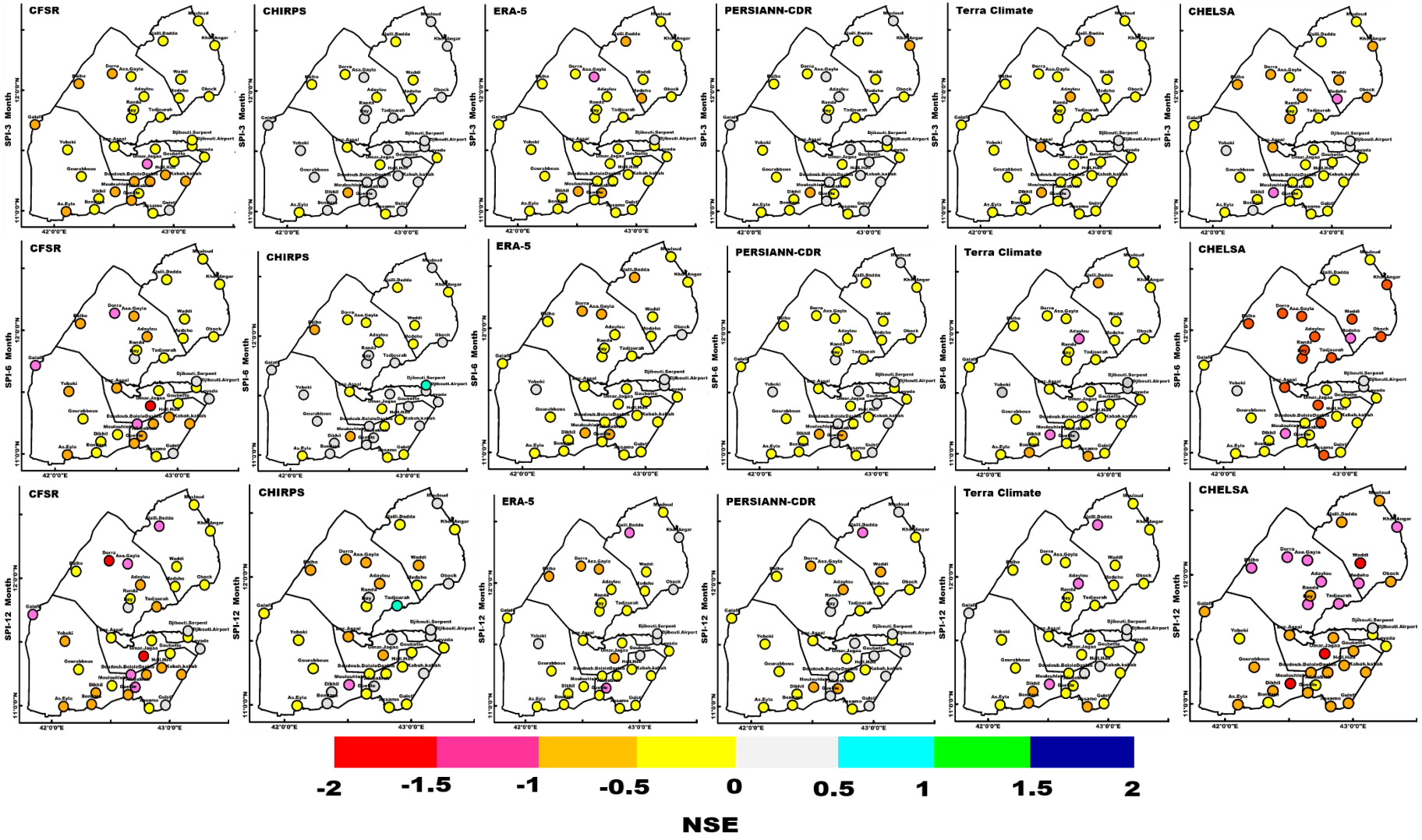

Figure 7. Spatial pattern of NSE of estimated monthly drought indices (3, 6, 12 month timescales) assessed from reanalysis products with the in situ observation over The Republic of Djibouti during 1983-2021.

3.3.2. Characteristics of regional Drought over the Republic of Djibouti

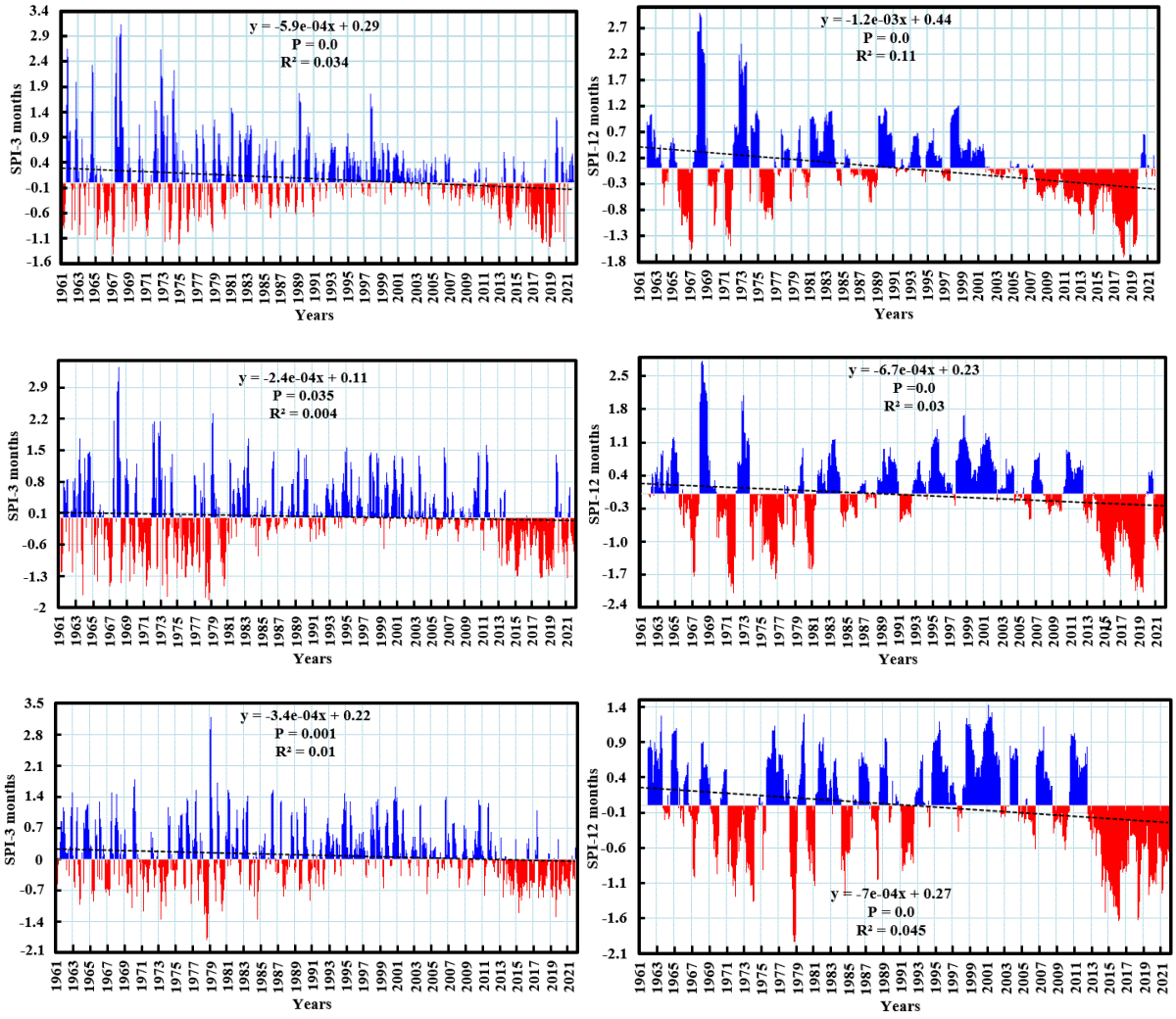

Figure 8. Linear trends of dry and wet events for SPI over three distinct climatic zones (Eastern, Center and Western), as presented in Table.

Table 9. The characteristics of a major dry and wet events (SPI≤-1, SPI ≥+1) of three different region in republic of Djibouti, 1961 to 2021.

Drought Characteristics	Severity	Duration	Intensity	Occurrence	Area (%)
Dry Event - EASTERN REGION					
SPI-3-months	-25.423	22	-1.156	3.005	49.667
SPI-6-months	-56.281	47	-1.197	6.421	50.812
SPI-12-months	-62.103	49	-1.267	6.694	52.344
Dry Event - CENTER REGION					
SPI-3-months	-62.103	49	-1.267	6.694	50.282
SPI-6-months	-116.391	84	-1.386	11.475	48.930
SPI-12-months	-135.366	91	-1.488	12.432	46.102
Dry Event - WESTERN REGION					
SPI-3-months	-22.863	18	-1.27	2.459	49.846
SPI-6-months	10.656	39	-1.242	5.328	48.882
SPI-12-months	-72.674	57	-1.275	7.787	45.787

Drought Characteristics	Severity	Duration	Intensity	Occurrence	Area (%)
Wet Event - EASTERN REGION					
SPI-3-months	85.589	52	1.646	7.104	50.333
SPI-6-months	95.417	61	1.564	8.333	49.188
SPI-12-months	88.71	56	1.584	7.65	47.656
Wet Event - CENTER REGION					
SPI-3-months	88.71	56	1.584	7.65	49.718
SPI-6-months	108.205	79	1.37	10.792	51.070
SPI-12-months	93.953	66	1.424	9.016	53.898
Wet Event - WESTERN REGION					
SPI-3-months	103.778	78	1.33	10.656	50.154
SPI-6-months	87.244	69	1.264	9.426	51.118
SPI-12-months	49.707	44	1.13	6.011	54.213

3.3.2. The drought Characteristics over the Republic of Djibouti, 1983-2021

La moyenne annuelle de l'indice SPI-3 et 12 de la sécheresse est présenté dans la figure 9. La sècheresse était extrême en 1968 et moderate en 1967, 1968, 1972 et 1973. Les années les plus humides sont observés durant 1967, 1968 et 1979 (Figure 9). Les années ou l'humidité est sévère sont observées en 1943, 1968, 1971, 1973, 2015, 2018 et 2019 (Figure 9).

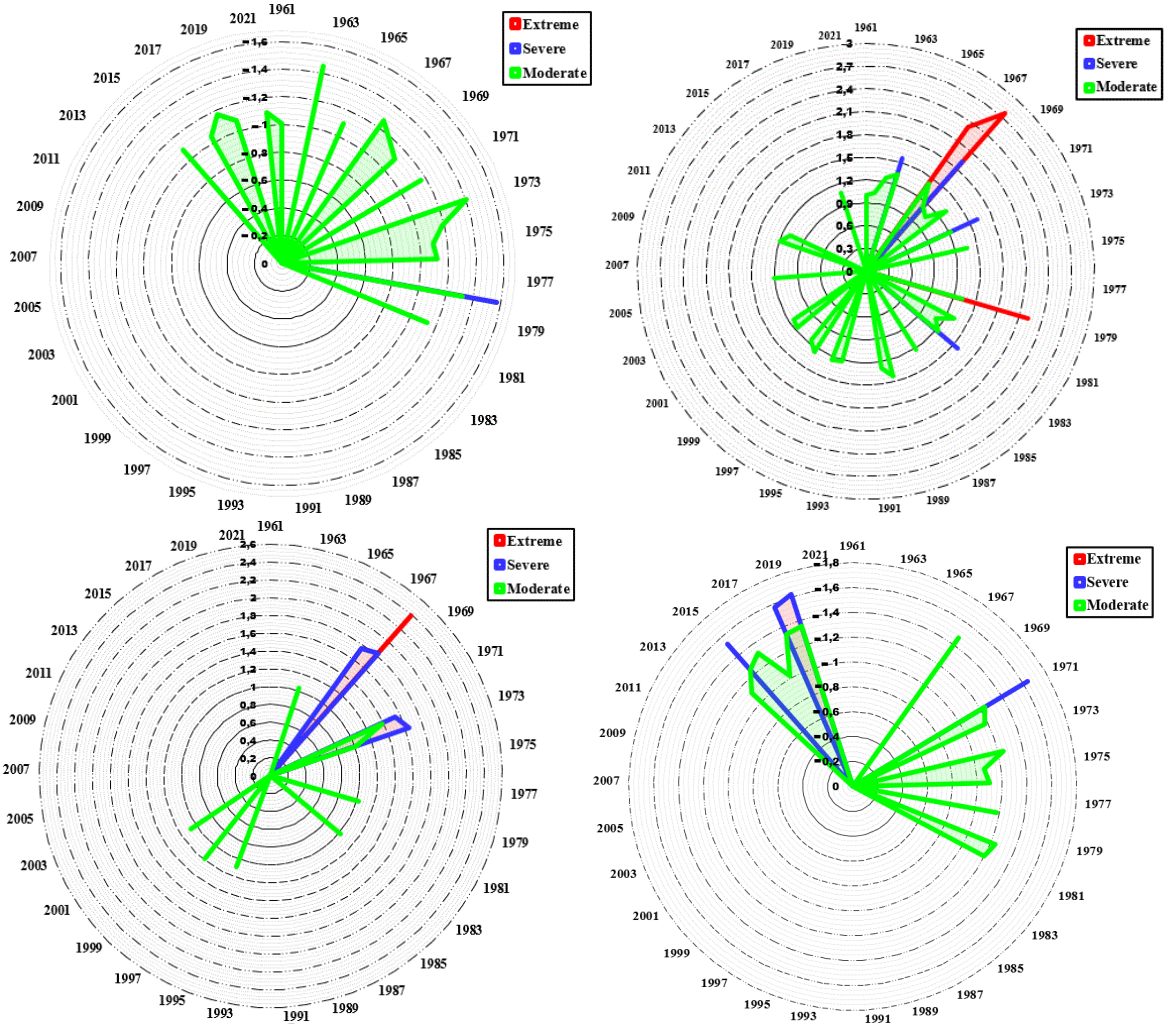

FIGURE 9. Evolution of the mean SPI for 3 and 12 month timescales for moderate, severe, and extreme drought and flood over the Republic of Djibouti from 1961 to 2021.

Le pourcentage de surface affecté par la sécheresse augmente plus en 2015 et 2018. Tandis que 1984, 1995 et 1999 à 2002, la sécheresse est de plus en plus faible sur le territoire de Djibouti.

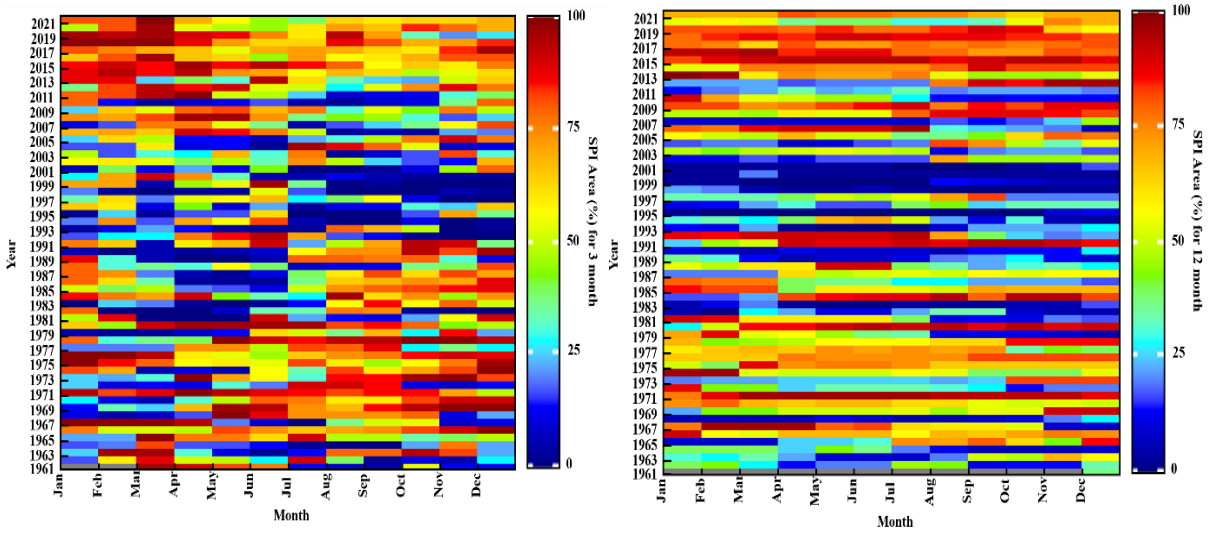

FIGURE 10. Temporal pattern of severity Drought with SPI 3 and 12 months.

La précision de chacune de produit satellitaire en comparaison avec les données observées est présenté dans la figure 11. Les produits CHELSA, ERA5 et CFSR sous-estiment les observations, contrairement CHIRPS. Le résultat montre que PERSIANN-CDR est proche de la variation de la sécheresse

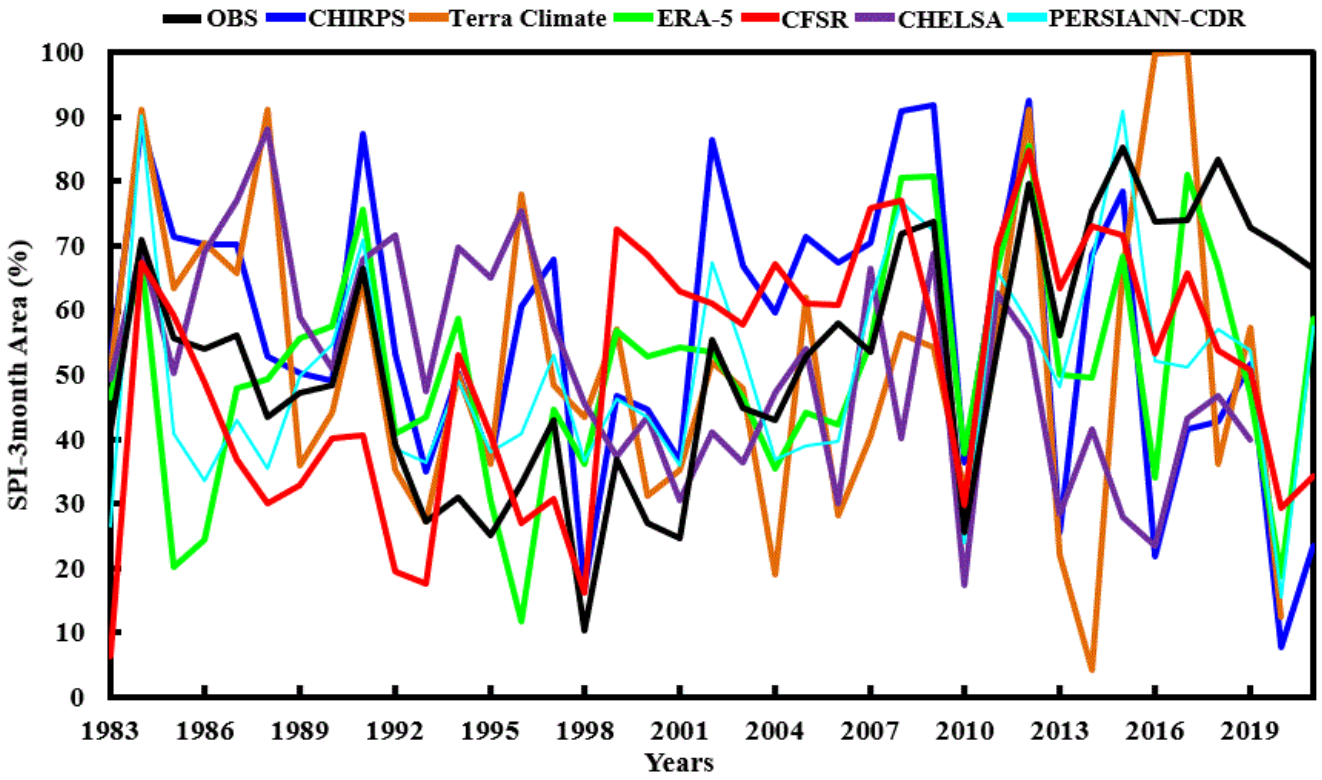
OBS
CHIRPS
Terra Climate
ERA-5
CFSR
CHELSA
PERSIANN-CDR
SPI-3month Area (%)
100
90
80
70
60
50
40
30
20
10
0
1983
1986
1989
1992
1995
1998
2001
2004
2007
2010
2013
2016
2019
Years

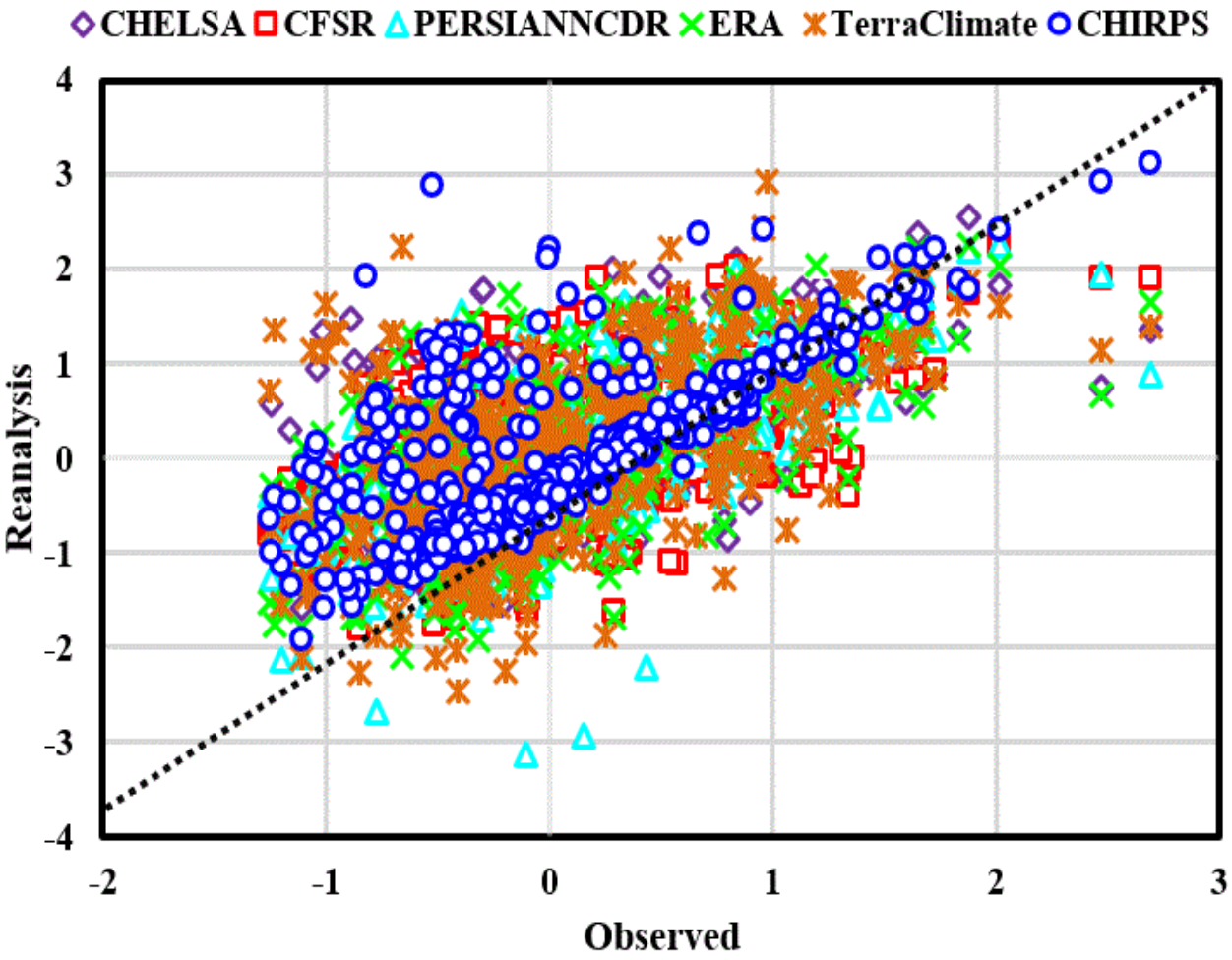

FIGURE 11. Times series illustrates the monthly drought areas derived from reanalysis products and in situ observation over the Republic of Djibouti for different timescale (scatterplots for drought severity, in the left)

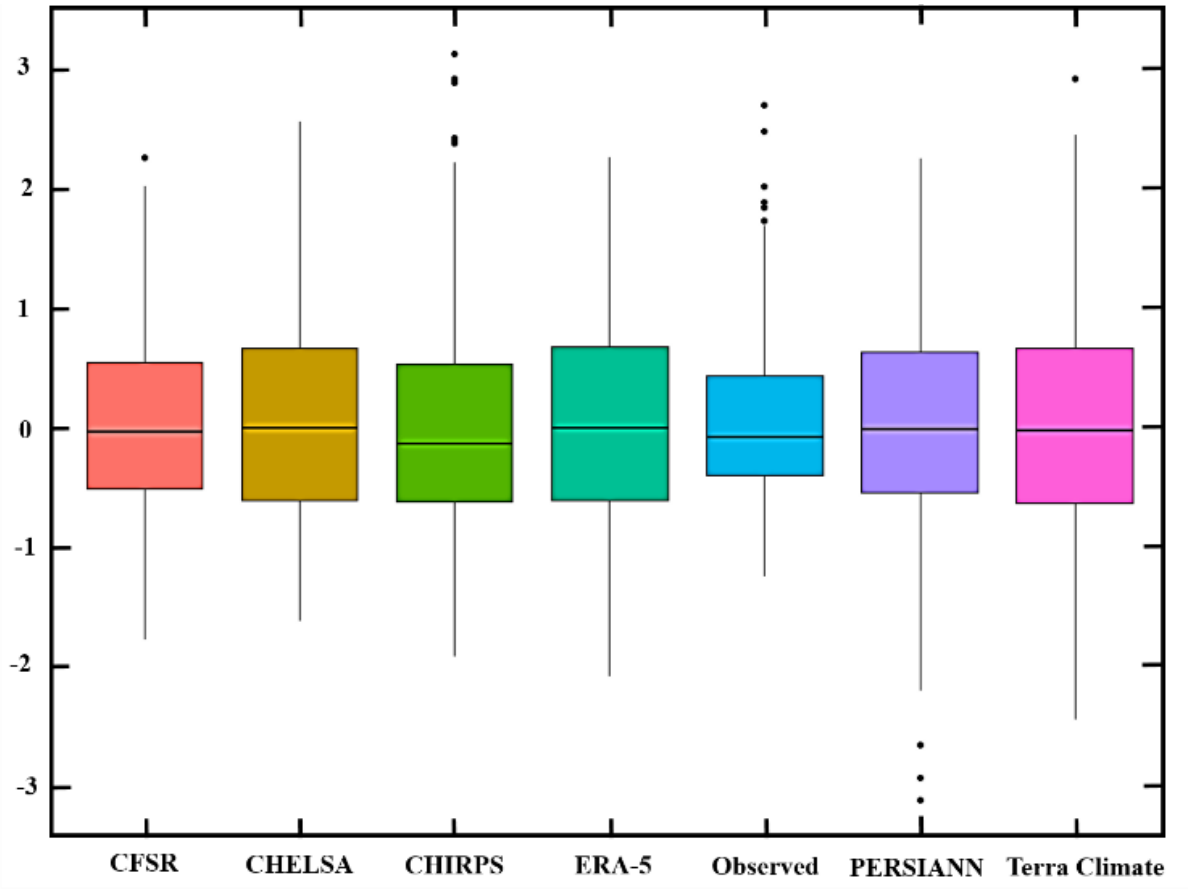

FIGURE 12. Boxplots presents the range of meteorological severity over during 1983-2021 based on SPI estimation derived from reanalysis and observation.

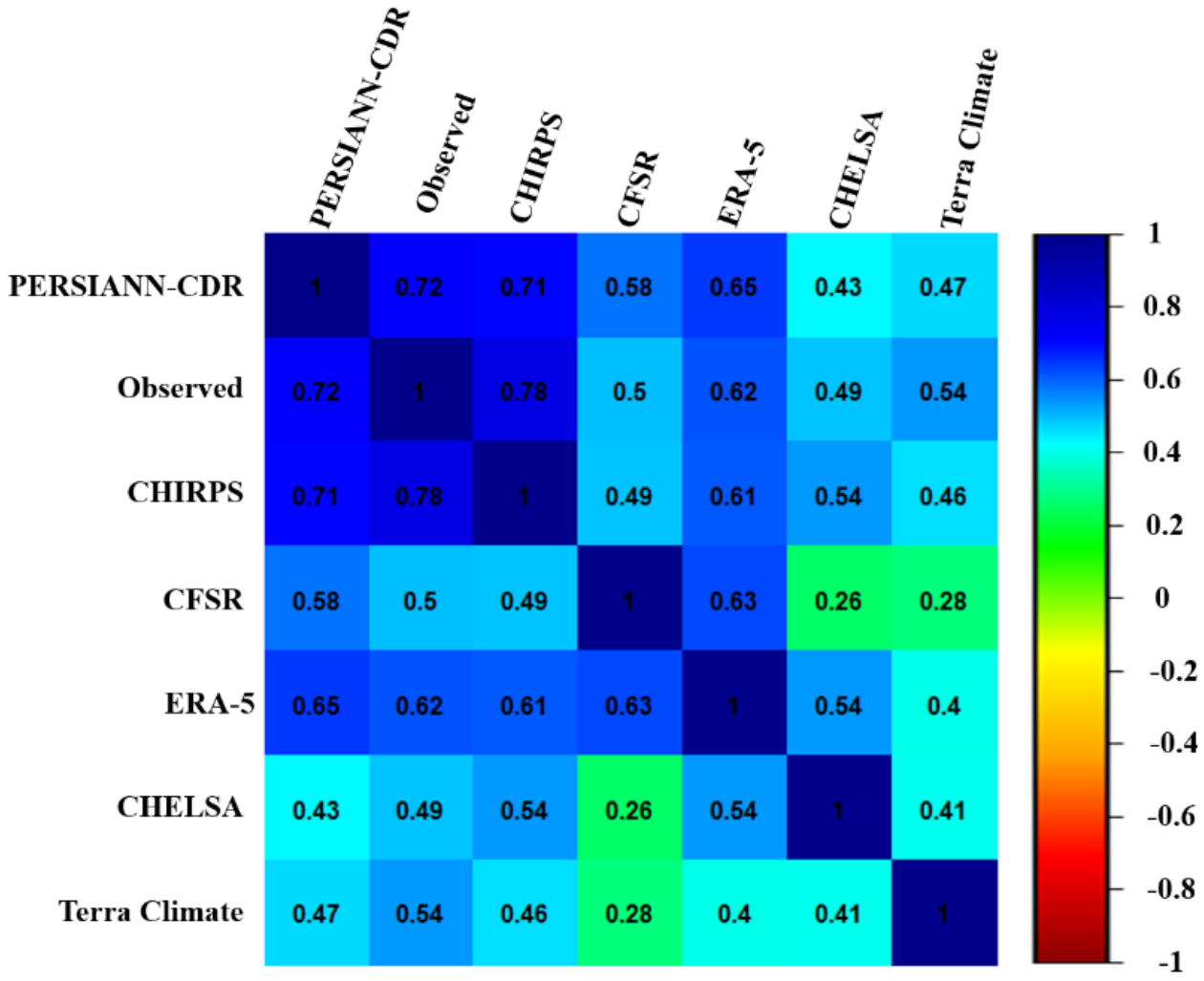

FIGURE 13. The Correlation coefficient matrix of the times series (1983-2021) estimated from SPI (3, 6, 12 months timescales) derived from reanalysis products compared with in situ observation over the Republic of Djibouti.

Table S1. Inter annual statistical parameters comparison of precipitation reanalysis products against ground based data at Djibouti-Airport station during 1983-2016

Station	Precipitation Product	N	CC	Slope	RMSE (mm)	BIAIS (mm)	Annual Rainfall (mm)
Djibouti-Airport	PERSIANN-CDR	403	0.551		25.6	4.75	193.77
	CHIRPS	408	0.506		25.71	-2.7	104.42
	ERA 5	408	0.724		26.3	13.51	298.95
	Terra Climate	408	0.592		23.88	-2.2	110.47
	CHELSA	408	0.827		24.08	7.38	225.43

Note: N is the number of available observations for monthly data. Significativity trend level *. **. ***

Table S2. Inter annual statistical parameters comparison of temperature reanalysis products against ground based data at Djibouti-Airport station during 1983-2016.

Station	Temperature Product		N	Slope	CC	RMSE (°C)	BIAIS (°C)	Average Annual Temperature (°C)
Djibouti-Airport	CHIRTS	T.max	408		0.958	1.635	-0.912	35.753
		T.min	408		0.938	6.205	-6.062	32.322
	ERA 5	T.max	408		0.976	5.273	5.145	29.696
		T.min	408		0.964	1.281	0.779	25.481
	Terra Climate	T.max	408		0.968	4.147	1.186	33.655
		T.min	408		0.951	1.167	-0.389	26.649
	CFS Reanalysis	T.max	408		0.945	4.92	0.632	34.209
		T.min	408		0.937	4.308	4.114	22.146

Note: N is the number of available observations for monthly data. Significativity trend level *. **. ***